Voronoi Diagrams for Parallel Halflines and Line Segments in Space *

Franz Aurenhammer[1], Bert Jüttler[2], and Günter Paulini[3]

1 **Institute for Theoretical Computer Science, University of Technology, Graz, Austria**
auren@igi.tugraz.at
2 **Institute of Applied Geometry, Johannes Kepler University, Linz, Austria**
bert.juettler@jku.at
3 **Institute for Theoretical Computer Science, University of Technology, Graz, Austria**
guenter.paulini@igi.tugraz.at

Abstract

We consider the Euclidean Voronoi diagram for a set of n parallel halflines in $\mathbb{R}^3$. A relation of this diagram to planar power diagrams is shown, and is used to analyze its geometric and topological properties. Moreover, an easy-to-implement space sweep algorithm is proposed that computes the Voronoi diagram for parallel halflines at logarithmic cost per face. Previously only an approximation algorithm for this problem was known. Our method of construction generalizes to Voronoi diagrams for parallel line segments, and to higher dimensions.

1998 ACM Subject Classification F.2.2 Nonnumerical Algorithms and Problems, G.2.1 Combinatorics

Keywords and phrases Voronoi diagram, line segments, space-sweep algorithm

Digital Object Identifier 10.4230/LIPIcs.ISAAC.2017.7

1 Introduction

The Voronoi diagram of a set of sites in Euclidean d-space $\mathbb{R}^d$ is a powerful and widely used geometric partitioning structure. It associates each site with the region of all points in $\mathbb{R}^d$ for which this site is closest among the given set. In the plane $\mathbb{R}^2$, many of the properties of Voronoi diagrams are well understood, also in generalized settings of various kinds; see e.g. [7].

Knowledge becomes quite sparse in dimensions larger than two, when sites of a shape more general than points are allowed. This concerns the structural as well as the algorithmic properties, and is already true for the seemingly harmless generalization from point sites to line segments. The combinatorial complexity of the Voronoi diagram for n line segments, and in particular, for n straight lines in $\mathbb{R}^d$ can be as large as $\Omega(n^{d-1})$, as has been shown in [4]. The only known upper bound follows from a general result in [17] on lower envelopes of hypersurfaces in $\mathbb{R}^{d+1}$ that represent the distance functions to the line segments, and is $O(n^{d+\varepsilon})$ for any $\varepsilon > 0$.

Even in $\mathbb{R}^3$, no better bounds than $\Omega(n^2)$ and $O(n^{3+\varepsilon})$, respectively, are known up to date. This may be partially due to the complicated shape of the arising bisector surfaces.

* This work was supported by Project I 1836-N15, Austria Science Fund (FWF)

They contain, among even more complex components, parabolic and hyperbolic patches, and can lead to a diagram of fairly complicated topological structure. Already for three straight lines as sites, the induced structure gets so intricate that a separate paper has been devoted to its exploration [12].

To make the problem more tractable, several restricted scenarios have been considered. For example, if the line segment sites are confined to have only constantly many orientations [15], then the size of the diagram reduces to $O(n^{2+\varepsilon})$. If, on the other hand, the underlying distance function is polyhedral and convex, then the diagram becomes piecewise-linear. The upper bound then can be tightened to $O(n^2\alpha(n)\log n)$ when the sites are straight lines [9], and to $O(n^{2+\varepsilon})$ when line segments and even constant-sized convex polyhedra are allowed as sites [14]. A practical algorithm for computing the medial axis of a nonconvex polytope in $\mathbb{R}^3$ under a convex polyhedral distance function is given in [3].

In the present note, we discuss a non-trivial special case for the Euclidean distance, namely, the case where all sites are parallel halflines in $\mathbb{R}^3$, being unbounded in the same direction. Apart from the theoretical interest, practical applications arise in certain problems in the drilling industry (mining exploitation, offshore drilling, hydraulics, etc.), as is reported by Adamou [1]. In particular, such Voronoi diagrams serve in the exploration of the nearest layers to avoid collision between wells and identifying unwanted plies. A related problem where these diagrams may be useful is approximate nearest-neighbor searching among a set of parallel line segments in $\mathbb{R}^3$, which has been studied in Emiris et al. [10].

The only known construction algorithm [1, 2] is algebraic and uses a box subdivision process. It produces a topologically correct approximation of the Voronoi diagram for parallel halflines; the runtime naturally depends on the accuracy of the approximation. (A related general approach, for planar Voronoi diagrams, is given in [11].) The algorithm we are going to present is exact, easy to implement (we have implemented and tested it on various inputs), and its runtime is output-sensitive. In particular, it runs at logarithmic cost per diagram face, extracts the correct topology of the diagram *without* manipulating any three-dimensional objects, and its most complex operation is solving a quadratic equation.

Our method is based on the insight that the diagram to be constructed is related to planar power diagrams, which are piecewise linear structures [5]. We describe this correspondence in Section 2, along with its structural implications. On the algorithmic side, a simple space-sweep algorithm is obtained in Section 3. Basically, a power diagram for fixed sites has to be updated under continuous changes of site weights. Section 4 studies the behavior of the trisector curves for the halfline Voronoi diagram, motivated by an attempt to reduce the $O(n^{2+\varepsilon})$ upper bound on its combinatorial complexity (which follows from the aforementioned result in [15]) to $O(n^2)$. Some extensions of our results are mentioned in Section 5. A preliminary version of this paper has appeared in [8].

2 Diagram

We start with a formal definition of the halfline Voronoi diagram. Let $H = \{h_1, \ldots, h_n\}$ be a set of parallel halflines in $\mathbb{R}^3$. We assume that each h_i is vertical (which is no loss of generality), and that each h_i is unbounded in negative z-direction (a restriction which is valid for the application mentioned before [1]). The upper endpoint of h_i is denoted by z_i. We call z_i the *tip* of h_i and, by slight abuse of notation, we will use z_i also to denote the z-coordinate of the tip. The distance of a point $x \in \mathbb{R}^3$ to a halfline h_i is defined as

$$d(x, h_i) = \min\{\delta(x, q) \mid q \in h_i\}$$

where δ denotes the Euclidean distance function. This distance is the normal distance of x to the supporting line, ℓ_i, of h_i, unless $d(x, h_i)$ is attained at the tip z_i. The *region* of a halfline in the Voronoi diagram, $\mathcal{V}(H)$, of H is given by

$$\mathrm{reg}(h_i) = \{x \in \mathbb{R}^3 \mid d(x, h_i) \leq d(x, h_j), \text{for all } j\}.$$

Regions are bounded by *bisectors*, B_{ij}, for pairs of halflines h_i, h_j, which are sets of points equidistant from two halflines. Let the respective tips satisfy $z_i \geq z_j$. Then B_{ij} is composed of three parts: a planar patch, contained in the (vertical) bisecting plane of the lines ℓ_i and ℓ_j, a piece of a parabolic cylinder equidistant from line ℓ_i and point z_j, and another planar patch in the bisecting plane of the points z_i and z_j. In the special case $z_i = z_j$, the bisector B_{ij} is just a vertical plane.

Concerning the parabolic bisector patch, note that its intersection with the (vertical) plane through h_i and h_j is the parabola defined by ℓ_i and z_j. Moreover, its intersection with any horizontal plane is a straight line. That is, the generators of the parabolic bisector patches are horizontal lines, which leads us to conclude a property that eases the analysis of the structure of $\mathcal{V}(H)$.

▶ **Observation 1.** *The intersection of B_{ij} with any horizontal plane is a straight line.*

Denote now by E^Δ the horizontal plane $z = \Delta$, and consider the lines $b_{ij} = B_{ij} \cap E^\Delta$. As bisectors intersect triple-wise in so-called *trisectors*, $t_{ijk} = B_{ij} \cap B_{ik} \cap B_{jk}$, the lines b_{ij}, b_{ik}, and b_{jk} concur in a common point (or are parallel), for any pairwise different indices i, j, k. This implies, by a result in [6], that the line system $(b_{ij})_{1 \leq i < j \leq n}$ is the set of *power lines* defined by n weighted points (that represent n circles) in E^Δ. A more direct argument for this fact follows from the lemma below.

▶ **Lemma 2.** *Consider the point $p_i = \ell_i \cap E^\Delta$, and assign the weight $w_i = -\max\{0, (\Delta - z_i)\}^2$ to it. For any $x \in E^\Delta$, we have $d(x, h_i)^2 = \delta(x, p_i)^2 - w_i$.*

In other words, the squared Euclidean distance of a point $x \in \mathbb{R}^3$ to the halfline h_i is the *power distance* [5] of x to the point p_i with weight w_i.

Proof. If E^Δ lies below z_i then $p_i \in h_i$ and $w_i = 0$, and the assertion is trivial. Otherwise, it follows from the Pythagorean theorem, because h_i is normal to E^Δ. ◀

Notice that the weight but not the position of p_i in E^Δ depends on Δ. By Lemma 2 we have the following geometric relation:

▶ **Theorem 3.** *For all values Δ, the sectional diagram $\mathcal{V}(H) \cap E^\Delta$ is identical to the power diagram of the points $p_1, \ldots, p_n$, for the weights w_i in Lemma 2.*

In particular, if the plane E^Δ lies below all tips then the Euclidean Voronoi diagram of $p_1, \ldots, p_n$ is obtained.

Figure 1 displays the trisector arcs of $\mathcal{V}(H)$ for a set H of 10 halflines. A corresponding sectional power diagram is shown in Figure 2.

Theorem 3 indicates that $\mathcal{V}(H)$ must have an assessable structure, which we study now in more detail. First of all, the weights w_i, when seen as functions $w_i(\Delta)$, are continuous. More precisely, $w_i(\Delta)$ is zero for $\Delta \leq z_i$, and decreases quadratically for $\Delta > z_i$.

We watch the interplay on E^Δ when Δ is increased from $-\infty$ to ∞. The power cells $C_i(\Delta) = \mathrm{reg}(h_i) \cap E^\Delta$ are convex polygons, whose vertices move continuously with Δ. For sufficiently small Δ, each cell $C_i(\Delta)$ is a planar Voronoi region, and therefore is non-empty.

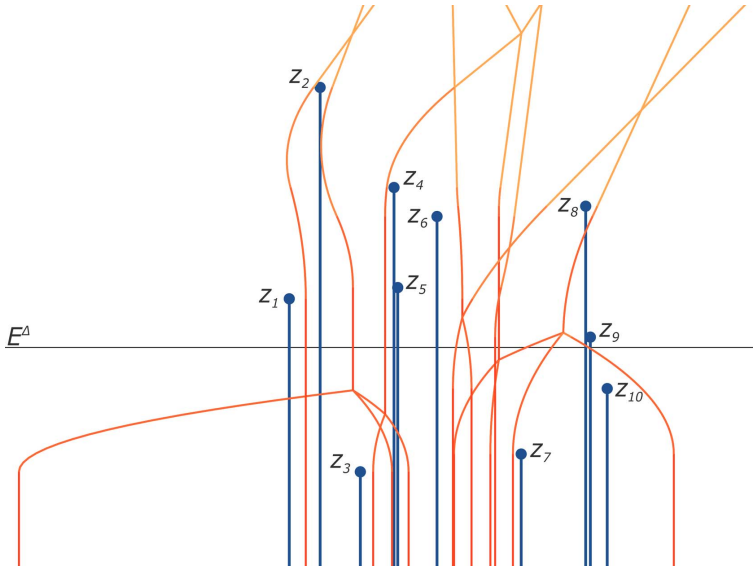

Figure 1 Halfline Voronoi diagram and some sectional plane E^Δ (projected view).

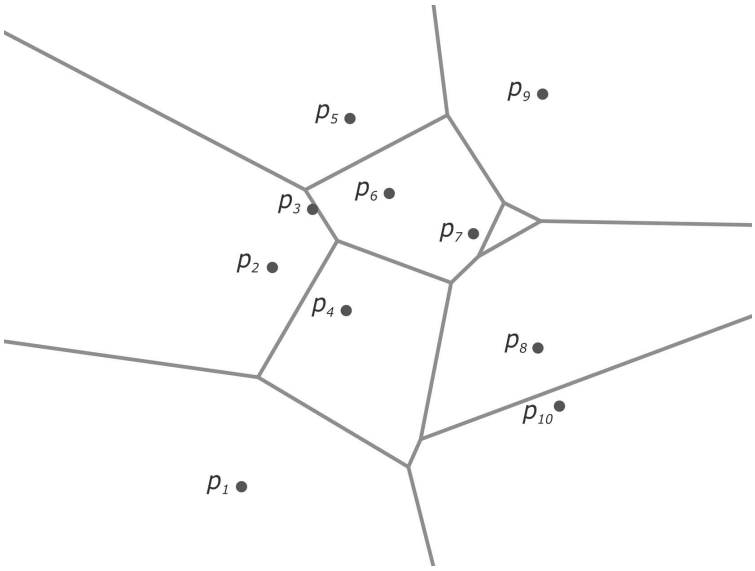

Figure 2 The sectional power diagram that corresponds to Figure 1.

Its edges first poise, and then move self-parallelly because $p_1, \ldots, p_n$ stay fixed and any power line for a pair of points p_i, p_j has to be perpendicular to the line segment $\overline{p_i p_j}$. Moreover, the movement of each single edge is always in a fixed direction, by the afore-mentioned shape of a bisector B_{ij}. So each point $x \in E^\Delta$ can enter or leave $C_i(\Delta)$ at most once. Also, if $C_i(\Delta)$ disappears from the diagram it cannot reappear, by the monotone movement of its edges. We summarize by stating the following observations on the regions of $\mathcal{V}(H)$.

▶ **Property 4.** *The intersection of $reg(h_i)$ with every vertical line is connected or empty. Moreover, $reg(h_i)$ is a connected set.*

Note that a power cell $C_i(\Delta)$ survives for $\Delta \to \infty$ if and only if the tip z_i appears on the *upper convex hull* of $\{h_1, \ldots, h_n\}$, that is, on that part of the convex hull of the point set $\{z_1, \ldots, z_n\}$ which is visible from $z = \infty$.

Unfortunately, Property 4 does not imply that the combinatorial size of $\mathrm{reg}(h_i)$ is $O(n)$: Although the number of bisectors B_{ij} that border $\mathrm{reg}(h_i)$ is trivially limited to $n-1$, a single bisector may define more than one *facet* (connected boundary patch) of $\mathrm{reg}(h_i)$. Indeed, there are multiple adjacencies between the regions in $\mathcal{V}(H)$ in general; see Section 4.

Let us now have a look at the Voronoi diagram $\mathcal{V}(\{h_i, h_j, h_k\})$ for only three halflines. The trisector curve t_{ijk} corresponds to a power diagram vertex $u^\Delta = t_{ijk} \cap E^\Delta$ for all Δ, unless the three points p_i, p_j, and p_k are collinear. (We exclude the latter case for the ease of description; it leads to $t_{ijk} = \emptyset$). This implies:

▶ **Property 5.** *Each trisector t_{ijk} is a connected curve, unbounded in both z-directions, and monotone with respect to z.*

In particular, t_{ijk} does not contain cycles. For pairwise different tip heights, the curve t_{ijk} is composed of 4 pieces, as can be easily verified: a halfline, two quadratic arcs, and another halfline. Therefore the algebraic degree of t_{ijk} is only two. Still, trisectors show a complicated intersection pattern in general. We will address this issue in Section 4.

3 Algorithm

We now turn to the algorithmic aspects of the halfline Voronoi diagramm $\mathcal{V}(H)$. Theorem 3 suggests a *space-sweep* algorithm that computes $\mathcal{V}(H)$ piece by piece, by moving a horizontal plane E^Δ in ascending z-direction. In fact, an entirely two-dimensional implementation is possible (and has been done by the authors), which avoids computing costly intersections of bisector surfaces in $\mathbb{R}^3$. Once the combinatorial structure of $\mathcal{V}(H)$ has been extracted, the bisector patches and trisector arcs that determine the geometry of $\mathcal{V}(H)$ can be 'filled in' in a final step.

The basic task is to maintain a power diagram for fixed points in the plane, under variation of their weights. The incidence structure of $\mathcal{V}(H)$ then can be inferred from the combinatorial changes that take place in the power diagram: When a power diagram edge appears (or disappears, respectively), then a facet of $\mathcal{V}(H)$ is born (or completed). Moreover, the collapse of a power cell signals the completion of a region in $\mathcal{V}(H)$.

To describe the combinatorial part of the algorithm in more detail, let $\mathrm{PD}(\Delta)$ be the power diagram for the points $p_1, \ldots, p_n$ with weights $w_1(\Delta), \ldots, w_n(\Delta)$, as defined in Section 2. We start with any value $\Delta < \min\{z_1, \ldots, z_n\}$, and initialize $\mathrm{PD}(\Delta)$ as the planar Voronoi diagram of the set $\{p_1, \ldots, p_n\}$.

There is only one type of *events* (z-values) where the power diagram can change. These are the anticipated life ends a_{ij} of its edges e_{ij}.

More specifically, a_{ij} is the z-value of the lowest intersection point above E^Δ of the respective two trisector curves t_{ijk} and t_{ijm}, which define the endpoints of e_{ij}. This value can be calculated in $O(1)$ time, by solving a single quadratic equation in the variable z, for each of the 5 intervals given by z_i, z_j, z_k, z_m. (These intervals determine the weights to be used.) In the diagram $\mathrm{PD}(a_{ij})$, an update of constant complexity has to be performed. This update is either a 'flip' that replaces the edge e_{ij} by the edge e_{km} (and a facet of the halfline Voronoi diagram $\mathcal{V}(H)$ in the bisector B_{ij} gets completed), or a collapse of a triangular cell incident to the edge e_{ij}, say $C_i(a_{ij})$ (and the region $\mathrm{reg}(h_i)$ of $\mathcal{V}(H)$ gets completed).

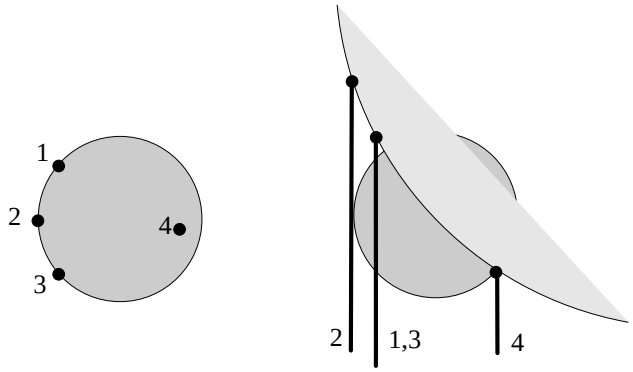

Figure 3 Two spheres touching the same set of 4 halflines. (Thanks go to Peter Widmayer's group for pointing us to this example.)

Notice that the tips z_i of the halflines h_i do not lead to combinatorial changes in $\mathrm{PD}(z_i)$. They only alter the speeds of the edges in the power cell $C_i(z_i)$. This information is already incorporated in the trisector intersection task above.

We use a priority queue organized by z-values to maintain the order of events. Only $O(n)$ entries need to be stored at a time, by the linear number of edges in a power diagram of n weighted points [5]. The next event to be performed then is accessible in $O(\log n)$ time. Moreover, the total number of entries a_{ij} is bounded by the number of facets of $\mathcal{V}(H)$.

Note finally that the numbers of facets, arcs, and nodes of $\mathcal{V}(H)$ are linearly related: A region in $\mathcal{V}(H)$ with f facets has $O(f)$ arcs and nodes by the Euler characteristic, because the degree of its nodes is at least 3. We conclude a main result of this paper:

▶ **Theorem 6.** *The halfline Voronoi diagram $\mathcal{V}(H)$ can be computed in $O(k \log n)$ time and $O(k)$ space, where the number k of faces is bounded by $O(n^{2+\varepsilon})$.*

4 Trisectors

The combinatorial size of $\mathcal{V}(H)$ tends to be near-linear for many data, as has been observed in our experiments. Thus our output-sensitive algorithm in Section 3 can be expected to run fast in practice. On the other hand, $\mathcal{V}(H)$ can attain a complexity of $\Omega(n^2)$, for example, when the tips z_i are arranged like in an $\Theta(n^2)$ worst-case example for the Voronoi diagram of n point sites in $\mathbb{R}^3$; see e.g. [13]. This almost matches the upper bound of $O(n^{2+\varepsilon})$ for $\mathcal{V}(H)$, which follows from the more general bound in [15]; see Section 1. Proving a possible quadratic upper bound is complicated by the fact that the trisector curves of $\mathcal{V}(H)$ do not behave like pseudo-lines. Let us comment on this fact and its consequences.

For the halfline h_L with lowest tip, its region is always convex; all the bisectors B_{Lj} either 'bend' towards h_L or are vertical planes. If the size of $\mathrm{reg}(h_L)$ can be shown to be $O(n)$, then an insertion argument for regions in ascending order of tip heights implies an overall $O(n^2)$ diagram size. Unfortunately, two trisector curves on the boundary of $\mathrm{reg}(h_L)$ can intersect in more than one point, such that the result in [16] on the linear size of surface envelopes does not apply to $\mathrm{reg}(h_L)$.

To see an example with two intersection points, consider four halflines h_1, h_2, h_3, and h_4 arranged as is illustrated in Figure 3, from the top view (left) and from the front view (right), respectively. The two trisector curves t_{123} and t_{124} (and two others) concur in a point x, if and only if there exists a sphere centered at x that simultaneously touches all four halflines. There are two such spheres, a smaller one resting on the tip of the rightmost halfline, and a bigger one passing through all four tips.

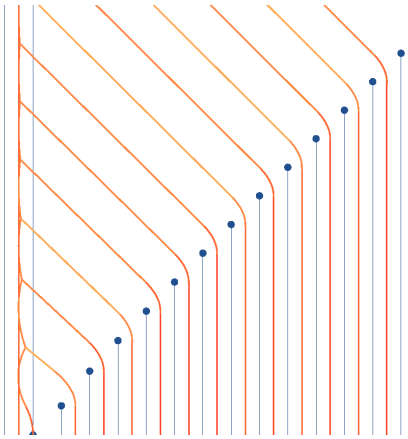

Figure 4 Two very high tips and a tip of height zero on the left, followed by $n-3$ tips of (roughly) linearly increasing heights.

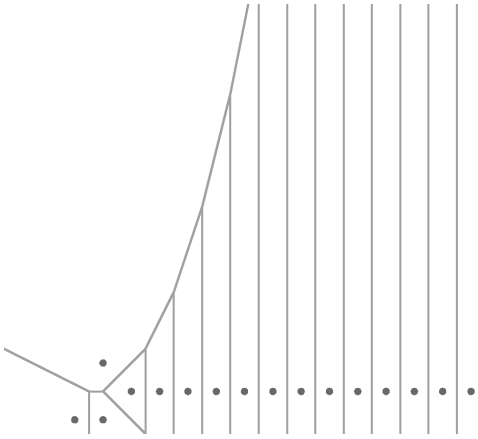

Figure 5 Power diagram for the lowest sectional plane, positioned at the bottom in Figure 4.

The trisectors defined by 4 halflines can have at most 3 intersection points, by a simple algebraic case analysis. This bound is actually attained, and even worse, there are constellations of n halflines for any $n \geq 4$ where every quadruple of related trisectors shows such an intersection behavior. For instance, this happens when the n tips are chosen to lie on the modified moment curve

$$M(t) = \begin{pmatrix} t \\ t^2 \\ tn2^t \end{pmatrix}, \text{ for } 1 \leq t \leq n.$$

As another approach to proving a quadratic upper bound for $\mathcal{V}(H)$, one can try to bound the overall number of edges that appear in the power diagram $\mathrm{PD}(\Delta)$ for varying Δ. This quantity describes the number of facets of $\mathcal{V}(H)$. There are $\binom{n}{2}$ potential power edges. However, once having disappeared, an edge between the same two power cells can appear again. In fact, this can happen a linear number of times: From the trisector pattern in Figure 4 it can be seen that the small horizontal power edge in Figure 5 (left lower corner) will vanish and reappear $n-3$ times when the sectional plane is raised up.

Stated differently, a fixed bisector B_{ij} can define $\Omega(n)$ facets where the two regions $\mathrm{reg}(h_i)$ and $\mathrm{reg}(h_j)$ are adjacent. On the other hand, edge speeds in $\mathrm{PD}(\Delta)$ are not arbitrary: Starting with 0, the speed of an edge increases at constant acceleration, until it stays constant forever. Thus a local multiple appearence of several edges might exclude some related power lines from contributing edges in the future. However, we found an example with 6 points where each of the $\binom{6}{2} - 6 = 9$ bounded power edges they define appears at least twice.

By the relationship between power diagrams and convex hulls (see e.g. [7]), the problem above can be transformed into a dynamic convex hull problem in $\mathbb{R}^3$. Starting from the paraboloid of revolution $z = x^2 + y^2$ at different times, n points move upwards vertically and at constant accelerations. The question of interest is now to bound the number of combinatorial changes that occur on their convex hull.

5 Extensions

The results of this paper can be extended in two different ways. One concerns the Voronoi diagram of parallel line segments that are bounded in *both* directions.

Lemma 2 generalizes straightforwardly to this case, such that Theorem 3 still holds. However, the resulting space-sweep algorithm now has to deal with the detection of new regions because, in general, not all of them will be witnessed by a power cell in the diagram $\mathrm{PD}(\Delta)$ for small Δ. Detection of new power cells cannot be done locally, unless involved data structures are maintained during the updates that occur in $\mathrm{PD}(\Delta)$ when Δ is increased.

A simple solution is to *insert* the input line segments $s_1, s_2, \ldots, s_n$ one by one, thereby using the space-sweep algorithm of Section 3. This is possible, because the region of a segment is always connected, even in the non-parallel case.[1] Initially, for those segments s_j which are unbounded in negative z-direction, the Voronoi diagram is constructed as before. If there are no such segments, we start with the Voronoi diagram of $\{s_1, s_2\}$, which just consists of the bisector of these two segments. An insertion step in the current diagram $\mathcal{V}$ then proceeds as follows:

Let s_i, for $i \geq 3$, be the line segment to be inserted. Choose a value of Δ where the corresponding point p_i has a non-empty cell in the power diagram, $\mathrm{PD}'(\Delta)$, for the weighted points whose segments have been inserted so far. (Clearly, the z-value of the midpoint of s_i is a valid choice.) Construct the power cell $C_i(\Delta)$ by insertion into $\mathrm{PD}'(\Delta)$, in $O(n)$ time. Now, starting from Δ in both z-directions, compute the Voronoi region of s_i and incooporate it into the diagram $\mathcal{V}$, by maintaining $C_i(\Delta)$ during two space sweeps. The parts of $\mathcal{V}$ that have to be deleted in this process can be identified on the fly. By adapting the runtime arguments given in Section 3, we obtain:

▶ **Lemma 7.** *Let f be the number of facets of the region of line segment s_i at the stage of its processing. Then s_i can be inserted in $O(f \log n)$ time.*

While the insertion of a single region thus can be done efficiently, the overall time for constructing the Voronoi diagram for parallel line segments can vary strongly, depending on the shapes of the regions and the insertion order. Unfortunately, no non-trivial upper bounds on the size of a region are known; the combinatorial complexity of the entire diagram is $O(n^{2+\varepsilon})$, by the results in [15]. In particular, the construction algorithm is not output-sentive any more. It still performs quite well in practice (if the search for a starting edge

[1] In particular, each point of a region is visible from its defining segment, like the two-dimensional case.

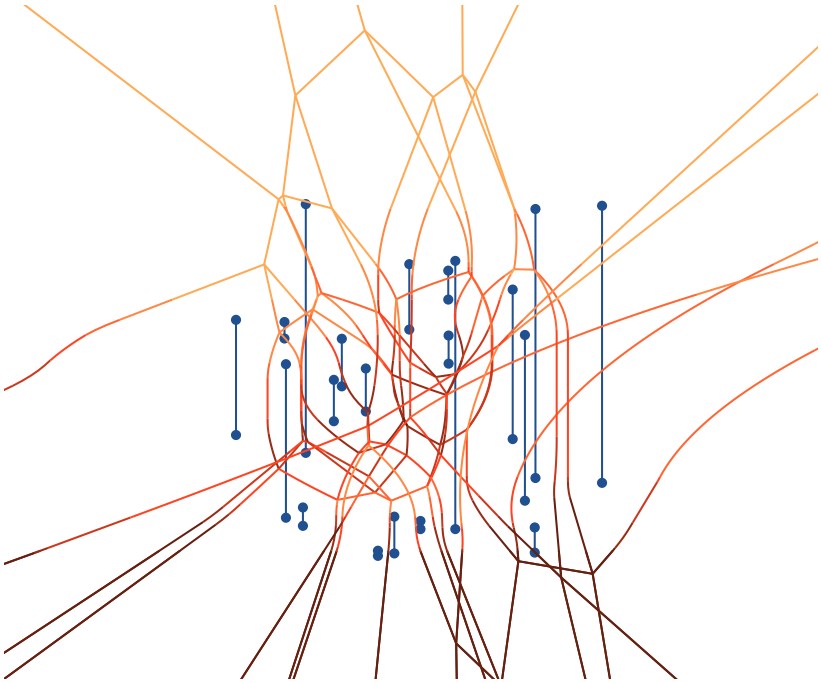

Figure 6 The Voronoi diagram for a set of 20 vertical line segments in 3-space

for $C_i(\Delta)$ is implemented efficiently), as we could observe in our experiments. Figure 6 gives an illustration of the output.

Our method of construction also generalizes to higher dimensions, as the geometric relations in Lemma 2 and Theorem 3 are dimension-independent. For example, to compute the Voronoi diagram of n vertical halflines in $\mathbb{R}^4$, a space-sweep algorithm that maintains a power diagram in a horizontal hyperplane E^Δ of $\mathbb{R}^4$ can be applied. This power diagram is a cell complex consisting of at most n convex 3-dimensional cells. For increasing Δ, the combinatorial changes (events) in this cell complex in E^Δ can be detected by the collapses of its edges. These edges correspond to 2-dimensional faces in the desired 4-dimensional Voronoi diagram, $\mathcal{V}$. That is, the sweep algorithm constructs the diagram $\mathcal{V}$ 2-face by 2-face. Thereby, a simultaneous collapse of 3 edges indicates the completion of a 3-face (facet) of $\mathcal{V}$, and a simultaneous collapse of 6 edges witnesses the completion of a region of $\mathcal{V}$ (in the generic case).

In this way, the topological structure of $\mathcal{V}$ is computed in an output-sensitive manner, namely, in $O(\log n)$ time per 2-face. The same approach works in arbitrary fixed dimensions, where the halfline Voronoi diagram in $\mathbb{R}^d$ can be derived from a dynamically changing power diagram in $\mathbb{R}^{d-1}$. We refrain from describing the details which get more involved rapidly.

▶ **Theorem 8.** *For constant d, let H be a set of n parallel halflines in $\mathbb{R}^d$ that are unbounded in the same direction. If the Voronoi diagram of H is of combinatorial size K, then it can be computed in $O(K \log n)$ time and $O(K)$ space.*

References

1 I. Adamou. Curvas y superficies bisectrices y diagrama de Voronoi de una familia finita de semirrectas paralelas end R^3. Ph.D. thesis, Department of Mathematics, University of Cantabria, Spain, 2013.

2 I. Adamou., M. Fioravanti, L. Gonzalez-Vega, B. Mourrain. Bisectors and Voronoi diagram of a family of parallel half-lines. In: SAGA-Advances in ShApes, Geometry, and Algebra, Springer Verlag, 2014, 241–279.

3 O. Aichholzer, W. Aigner, F. Aurenhammer, and B. Jüttler. Exact medial axis computation for triangulated solids with respect to piecewise linear metrics. *Proc. Curves and Surfaces 2011*, J.-D. Boissonnat et al. (eds.), Springer Lecture Notes in Computer Science 6920, 2011, 1–27.

4 B. Aronov. A lower bound on Voronoi diagram complexity. *Information Processing Letters* 83 (2002), 183–185.

5 F. Aurenhammer. Power diagrams: properties, algorithms and applications. *SIAM Journal on Computing* 16 (1987), 78–96.

6 F. Aurenhammer and H. Imai. Geometric relations among Voronoi diagrams. *Geometriae Dedicata* 27 (1988), 65–75.

7 F. Aurenhammer, R, Klein, and D.T. Lee. *Voronoi diagrams and Delaunay Triangulations*. World Scientific, Singapore, 2013.

8 F. Aurenhammer, G. Paulini, and B. Jüttler. Voronoi diagrams for parallel halflines in 3D. In *Proc. 32nd European Workshop on Computational Geometry*, 2016, 127-130.

9 L.P. Chew, K. Kedem, M. Sharir, B. Tagansky, and E. Welzl. Voronoi diagrams of lines in 3-space under polyhedral convex distance functions. *J. Algorithms* 29 (1998), 238–255.

10 I. Emiris, T. Malamatos, and E. Tsigaridas. Approximate nearest neighbor queries among parallel segments. *Proc. 26th European Workshop on Computational Geometry*, 2010.

11 I. Emiris, A. Mantzaflaris, B. Mourrain. Voronoi diagrams of algebraic distance fields. *Computer-Aided Design* 45 (2013), 511–516.

12 H. Everett, D. Lazard, S. Lazard, and M. Safey El Din. The Voronoi diagram of three lines. *Discrete & Computational Geometry* 42 (2009), 94–130.

13 S. Fortune. Voronoi diagrams and Delaunay triangulations. In: D.-Z. Du and F.K. Hwang (eds.), *Computing in Euclidean Geometry*, Lecture Notes Series on Computing 1, World Scientific, Singapore, 1992, 193–233.

14 V. Koltun and M. Sharir. Polyhedral Voronoi diagrams of polyhedra in three dimensions. *Discrete & Computational Geometry* 31 (2002), 83–124.

15 V. Koltun and M. Sharir. Three-dimensional Euclidean Voronoi diagrams of lines with a fixed number of orientations. *SIAM Journal on Computing* 32 (2003), 616–642.

16 J. Schwartz and M. Sharir. On the two-dimensional Davenport-Schinzel problem. *Journal of Symbolic Computation* 10 (1990), 371–393.

17 M. Sharir. Almost tight upper bounds for lower envelopes in higher dimensions. *Discrete & Computational Geometry* 12 (1994), 327–345.